INTERNATIONAL JOURNAL OF COMPUTERS COMMUNICATIONS & CONTROL
Online ISSN 1841-9844, ISSN-L 1841-9836, Volume: 19, Issue: 1, Month: February, Year: 2024
Article Number: 4xyz, https://doi.org/10.15837/ijccc.2024.1.4xyz

CCC Publications

Adaptive Backstepping Sliding Mode Fault-Tolerant Control of Quadrotor UAV in the presence of external disturbances, uncertainties, and Simultaneous Actuator and Sensor faults

A. Ezzara*, A.Y. Ouadine, H. Ayad

Abderrahim Ezzara*
LSEEET Laboratory, Department of Applied Physics
Faculty of Science and Technology, Cadi Ayyad University, Marrakesh, Morocco
*Corresponding author: abderrahim.ezzara@ced.uca.ma

Ahmed Youssef Ouadine
Ecole Royale de l'Air, Marrakesh, Morocco
a.y.ouadine@gmail.com

Hassan Ayad
LSEEET Laboratory, Department of Applied Physics
Faculty of Science and Technology, Cadi Ayyad University, Marrakesh, Morocco
h.ayad@uca.ma

Abstract

This paper presents a new active fault-tolerant control strategy for quadrotor unmanned aerial vehicle against unknown external disturbances, system uncertainties, actuator faults, and sensor faults. Based on a quadrotor's nonlinear dynamic model, time-varying actuator and sensor faults are simultaneously estimated by a nonlinear unknown input observer, and to attenuate the effect of disturbances on fault estimation, a $\mathcal{H}_\infty$ performance index is used. Subsequently, a robust nonlinear adaptive backstepping sliding mode control technique is proposed to manage faults despite the presence of uncertainties and disturbances. Comparative simulations in MATLAB are provided to verify the effectiveness of the proposed strategy under different types of actuators and sensors in different scenarios.

Keywords: Active fault-tolerant control, quadrotor, actuator faults, sensor faults, external disturbances, uncertainties, nonlinear unknown input observer, backstepping, sliding mode control.

1 Introduction

In recent years, quadrotors as unmanned aerial vehicles (UAVs) have become increasingly vital in various fields. However, their widespread use also raises significant security concerns, including potential system failures and external disturbances. Ensuring quadrotors' reliability and resilience in the face of such challenges is critical for their effective operation in both civilian and military applications.

To address these challenges, fault-tolerant control (FTC) systems have become a focal point of research. Recent research has focused extensively on developing FTC strategies for quadrotors to address uncertainties, disturbances, actuator, and sensor faults. In [1], [2], [3], and [4] authors addresse actuator faults and/or disturbances and uncertainties for quadrotor; however, it lacks coverage of sensor faults and uncertainties. In [5], authors study the diagnosis and compensation for sensors and actuator constant faults in a quadrotor UAV in the presence of uncertainties and external disturbances using a feedback linearization technique and a nonlinear high-gain observer. A new FTC strategy for quadrotors under time-varying sensor faults and disturbances based on a disturbance observer and a non-singular fast terminal sliding mode algorithm is proposed in [6], excluding actuator faults and uncertainties. Finally, [7] introduces a robust backstepping control strategy that includes an adaptive observer for actuator faults, missing sensor faults, disturbances, and uncertainties. Other FTC strategies are proposed in [8], [9],[10].

Existing FTC approaches for quadrotor UAVs often ignore full fault coverage, especially regarding time-varying faults. Unlike previous strategies [1]-[10], neither has examined the handling of both time-varying sensor and actuator faults in the presence of uncertainties and external disturbances.

For fault estimation (FE), in [12], the authors suggest a novel nonlinear unknown input observer (NUIO), but they didn't take into consideration the effect of system uncertainties. In [13], [14], and [15], the proposed NUIO with partly decoupled disturbances must meet a rank condition, which limits its use to many real systems. In [16], authors didn't consider sensor faults. Inspired by [11], a novel NUIO with disturbance attenuation without rank requirement for the quadrotor system is proposed. This NUIO is integrated with backstepping and SMC techniques to handle time-varying external disturbances, uncertainties, actuator faults, and sensor faults. The strategy

The main contributions of this paper are: (1) the use of a complete nonlinear model of the quadrotor UAV taking into consideration different nonlinearities; (2) to estimate actuator and sensor faults simultaneously, a novel NUIO is developed without any rank requirement in the system model in the presence of uncertainties and external disturbances; (3) using a linear matrix inequality (LMI) formulation, the observer design problem is solved using H_∞ optimization; (4) using the NUIO-based FE, an adaptive backstepping sliding mode FTC controller is constructed; (5) in addition to parametric uncertainties, wind disturbances, and noise, different time-varying additive and multiplicative actuator and sensor faults types are taking into account.

The remainder of this study is organized as follows: Section II provides a description of the quadrotor nonlinear dynamic model. Various actuator and sensor fault types are modeled in this section. In Section III, using the H_∞ optimization, a NUIO is constructed to simultaneously estimate the actuator and sensor faults. Section IV provides a robust ABSMC strategy to handle system failure effects. Finally, Section V shows a validation of the proposed FTC using MATLAB simulations.

2 Quadrotor Nonlinear Dynamical modeling

2.1 Quadrotor dynamical modeling

The quadrotor dynamical model can be derived using the Newton-Euler formalism. Let's introduce two reference frames, let E (O, X, Y, Z) designate an inertial frame, and B (o, x, y, z) designate a frame permanently coupled to the quadrotor body as illustrated in Figure 1. Both of them are assumed to be at the center of gravity of the quadrotor UAV.

The absolute position of the quadrotor may be obtained by the three coordinates (x,y,z) and its attitude by the three Euler's angles, respectively roll ϕ, pitch θ, and yaw ψ.

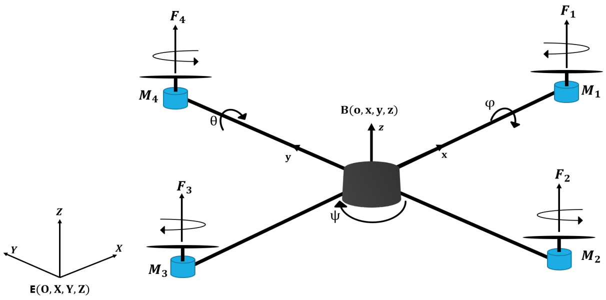

Figure 1: Quadrotor configuration

The quadrotor's dynamic model, which considers the drag forces, aerodynamic friction torques, and torques due to the gyroscopic effects, is given as in [17] by:

$$\ddot{\phi} = \frac{1}{I_x}\left(\dot{\theta}\dot{\psi}(I_y - I_z) - K_{fax}\dot{\phi}^2 - J_r\overline{\Omega}\dot{\theta} + dU_2\right) \tag{1a}$$

$$\ddot{\theta} = \frac{1}{I_y}\left(\dot{\phi}\dot{\psi}(I_z - I_x) - K_{fay}\dot{\theta}^2 + J_r\overline{\Omega}\dot{\phi} + dU_3\right) \tag{1b}$$

$$\ddot{\psi} = \frac{1}{I_z}\left(\dot{\theta}\dot{\phi}(I_x - I_y) - K_{faz}\dot{\psi}^2 + U_4\right) \tag{1c}$$

$$\ddot{x} = \frac{1}{m}\left((C\phi S\theta C\psi + S\phi S\psi)U_1 - K_{ftx}\dot{x}\right) \tag{1d}$$

$$\ddot{y} = \frac{1}{m}\left((C\phi S\theta S\psi - S\phi C\psi)U_1 - K_{fty}\dot{y}\right) \tag{1e}$$

$$\ddot{z} = \frac{1}{m}\left(C\phi C\theta U_1 - K_{ftz}\dot{z}\right) - g \tag{1f}$$

where C is the trigonometrical function cosine, and S is the function sine, m is the total mass of the quadrotor, g is the gravity acceleration constant, I_x, I_y, and I_z are the constants inertia, K_{ftx}, K_{fty}, and K_{ftz} are the translation drag coefficients, K_{fax}, K_{fay}, and K_{faz} are the coefficients of aerodynamic friction around X, Y, and Z, d is the distance between the center of mass of the quadrotor and the rotation axis of the propellers, J_r is the rotor inertia, $\overline{\Omega}$ represents the disturbance caused by the rotor unbalance, U_1, U_2, U_3, and U_4 represent the quadrotor control inputs.

Based on the angular speeds of the four rotors, the control inputs and the disturbance $\overline{\Omega}$ are expressed as follows:

$$\begin{bmatrix} U_1 \\ U_2 \\ U_3 \\ U_4 \end{bmatrix} = \begin{bmatrix} K_p & K_p & K_p & K_p \\ -K_p & 0 & K_p & 0 \\ 0 & -K_p & 0 & K_p \\ K_d & -K_d & K_d & -K_d \end{bmatrix} \begin{bmatrix} \omega_1^2 \\ \omega_2^2 \\ \omega_3^2 \\ \omega_4^2 \end{bmatrix} \tag{2}$$

$$\bar{\Omega} = \omega_1 - \omega_2 + \omega_3 - \omega_4 \tag{3}$$

where K_p is the lift coefficient, K_d is the drag coefficient, and ω_i for $i \in \{1, 2, 3, 4\}$ are the angular rotor speeds.

The control inputs remain restricted by the motors' maximum rotational speeds $\omega_{\max}$, which are illustrative of their physical constraints:

$$\begin{aligned} 0 \le U_1 &\le 4K_p\omega_{\max}^2 \\ -K_p\omega_{\max}^2 \le U_2 &\le K_p\omega_{\max}^2 \\ -K_p\omega_{\max}^2 \le U_3 &\le K_p\omega_{\max}^2 \\ -2K_d\omega_{\max}^2 \le U_4 &\le 2K_d\omega_{\max}^2 \end{aligned} \tag{4}$$

From the equations (1d) to (1f), we can extract the expressions of the nonholonomic constraints :

$$\tan\theta = \frac{(\ddot{x} + \frac{K_{ftx}}{m}\dot{x})C_\psi + (\ddot{y} + \frac{K_{fty}}{m}\dot{y})S_\psi}{\ddot{z} + g + \frac{K_{ftz}}{m}\dot{z}} \tag{5a}$$

$$\sin\phi = \frac{(\ddot{x} + \frac{K_{ftx}}{m}\dot{x})S_\psi - (\ddot{y} + \frac{K_{fty}}{m}\dot{y})C_\psi}{\sqrt{(\ddot{x} + \frac{K_{ftx}}{m}\dot{x})^2 + (\ddot{y} + \frac{K_{fty}}{m}\dot{y})^2 + (\ddot{z} + g + \frac{K_{ftz}}{m}\dot{z})^2}} \tag{5b}$$

Nonholonomic constraints will be used to produce the desired roll (ϕ_d) and pitch (θ_d).

2.2 Disturbaces, uncertainties, and faults modeling

To simulate the effect of wind disturbances, the Von Karman model will be used in this paper [18, 19, 20]. Wind disturbances will be noted $d_0(t)$ in the rest of this paper and given by:

$$d_0 = \left[d_\phi, d_\theta, d_\psi, d_x, d_y, d_z,\right]^T \tag{6}$$

where d_ϕ, d_θ, and d_ψ represents the disturbance affecting the quadrotor's attitude. And d_x, d_y, and d_z are the disturbances along the X, Y and Z axes, respectively.

We consider additional parameter uncertainties of the quadrotor model on the translation drag coefficients K_{ftx}, K_{fty}, and K_{ftz}, and the aerodynamic friction coefficients K_{fax}, K_{fay}, and K_{faz}. Based on the system model given by (1), the uncertainties effect can be expressed as follows:

$$\begin{aligned} \xi_\phi &= -\frac{\Delta K_{fax}}{I_x}\dot{\phi}^2, & \xi_\theta &= -\frac{\Delta K_{fay}}{I_y}\dot{\theta}^2, & \xi_\psi &= -\frac{\Delta K_{faz}}{I_z}\dot{\psi}^2, \\ \xi_x &= -\frac{\Delta K_{ftx}}{m}\dot{x}, & \xi_y &= -\frac{\Delta K_{fty}}{m}\dot{y}, & \xi_z &= -\frac{\Delta K_{ftz}}{m}\dot{z} \end{aligned} \tag{7}$$

where ΔK_{fax}, ΔK_{fay}, ΔK_{faz}, ΔK_{ftx}, ΔK_{fty}, and ΔK_{ftz} represent the uncertainties of K_{fax}, K_{fay}, K_{faz}, K_{ftx}, K_{fty}, and K_{ftz} respectively. The uncertainty vector will be noted $\xi(x,t)$ and given by $\xi = \left[\xi_\phi, \xi_\theta, \xi_\psi, \xi_x, \xi_y, \xi_z\right]^T$.

Common actuator faults include Bias fault, Loss of Effectiveness (LOE) fault, and Actuator Stuck fault [21, 22]. The combined equation for these faults can be described using:

$$f_a(t) = -\epsilon u(t) + f_{a0}(t) \tag{8}$$

where f_a is the actuator fault, u denotes the system control input, $\epsilon \in [0,1]$ denotes the actuator gain variation coefficient, and f_{a0} is an actuator fault function, and $f_a = \left[f_{a1}, f_{a2}, f_{a3}, f_{a4}\right]^T$.

Common sensor faults include bias fault, drift fault, loss of effectiveness (LOE), and stuck sensor fault [23, 24]. The combined equation for these faults can be described using:

$$f_s(t) = -\rho y(t) + f_{s0}(t) \tag{9}$$

where f_s is the sensor fault, y denotes system output, $\rho \in [0,1]$ denotes the sensor gain variation coefficient, and f_{s0} is a sensor fault function, and $f_s = \left[f_{s1}, f_{s2}, f_{s3}, f_{s4}, f_{s5}, f_{s5}\right]^T$.

2.3 Complete nonlinear quadrotor dynamic model

Let's define the system's state vector given by:

$$x = [x_1, \dots, x_{12}]^T = [\phi, \dot{\phi}, \theta, \dot{\theta}, \psi, \dot{\psi}, x, \dot{x}, y, \dot{y}, z, \dot{z}]^T \tag{10}$$

The system output vector is given by:

$$y = [x_1, x_2 - f_{s1}, x_3, x_4 - f_{s2}, x_5, x_6 - f_{s3}, x_7, x_8 - f_{s4}, x_9, x_{10} - f_{s5}, x_{11}, x_{12} - f_{s6}]^T \tag{11}$$

From equations (1) and considering uncertainties, disturbances, actuators, and sensor faults modeled above, we obtain the following state space model:

$$
\begin{aligned}
\dot{x}_1 &= x_2 \\
\dot{x}_2 &= a_1x_4x_6 + a_2x_2^2 + a_3\bar{\Omega}x_4 + b_1U_2 + f_{a1} + d_\phi + \xi_\phi \\
\dot{x}_3 &= x_4 \\
\dot{x}_4 &= a_4x_2x_6 + a_5x_4^2 + a_6\bar{\Omega}x_2 + b_2U_3 + f_{a2} + d_\theta + \xi_\theta \\
\dot{x}_5 &= x_6 \\
\dot{x}_6 &= a_7x_2x_4 + a_8x_6^2 + b_3U_4 + f_{a3} + d_\psi + \xi_\psi \\
\dot{x}_7 &= x_8 \\
\dot{x}_8 &= a_9x_8 + U_x\frac{U_1}{m} + d_x + \xi_x \\
\dot{x}_9 &= x_{10} \\
\dot{x}_{10} &= a_{10}x_{10} + U_y\frac{U_1}{m} + d_y + \xi_y \\
\dot{x}_{11} &= x_{12} \\
\dot{x}_{12} &= a_{11}x_{12} - g + \frac{\cos(x_1)\cos(x_3)}{m}U_1 + f_{a4} + d_z + \xi_z
\end{aligned}
\tag{12}
$$

where

$$
\begin{array}{lllll}
a_1 = \dfrac{I_y - I_z}{I_x}, & a_2 = -\dfrac{K_{fax}}{I_x}, & a_3 = -\dfrac{J_r}{I_x}, & a_4 = \dfrac{I_z - I_x}{I_y}, & a_5 = -\dfrac{K_{fay}}{I_y} \\
a_6 = \dfrac{J_r}{I_y}, & a_7 = \dfrac{I_x - I_y}{I_z}, & a_8 = -\dfrac{K_{faz}}{I_z}, & a_9 = -\dfrac{K_{ftx}}{m}, & a_{10} = -\dfrac{K_{fty}}{m} \\
a_{11} = -\dfrac{K_{ftz}}{m}, & b_1 = \dfrac{d}{I_x}, & b_2 = \dfrac{d}{I_y}, & b_3 = \dfrac{1}{I_z}. &
\end{array}
$$

3 NUIO-based FE design

The following state-space form can be employed to represent the complete model (12):

$$
\begin{aligned}
\dot{x}(t) &= Ax(t) + Bu(t) + \Phi(x,t) + F_af_a(t) + Dd(t) \\
y(t) &= Cx(t) + F_sf_s(t)
\end{aligned}
\tag{13}
$$

where $x \in \mathbb{R}^{12}$ and given by (10), $y \in \mathbb{R}^{12}$ and given by (11), the control input vector is given by $u = [U_1, U_2, U_3, U_4]^T$. $F_a \in \mathbb{R}^{12\times4}$ and $F_s \in \mathbb{R}^{12\times6}$ are known constant distribution matrices. $d \in \mathbb{R}^6$ represent lumped uncertainty that includes both external disturbances and system uncertainties. $\Phi \in \mathbb{R}^{12}$ is a continuous known nonlinear function vector. $A \in \mathbb{R}^{12\times12}$, $B \in \mathbb{R}^{12\times4}$, $C \in \mathbb{R}^{12\times12}$, and $D \in \mathbb{R}^{12\times6}$ are known constant matrices.

For the development of the considered observer, the following conditions must be satisfied [11]:

Assumption 1: The pair (A, C) is observable, the pair (A, B) is controllable, and $\mathrm{rank}(B, F_a) = \mathrm{rank}(B)$.

Assumption 2: The unknown input disturbances d is bounded with unknown upper bounds such that $d \in L_2[0, \infty)$.

Assumption 3: The faults f_a and f_s belong to $L_2[0, \infty)$, and f_a and f_s are continuously smooth with bounded first-time derivatives.

Assumption 4: $\Phi(x, t)$ satisfies the Lipschitz property with respect to x, such that:

$$
\|\Phi(x,t) - \Phi(\hat{x},t)\| \leq L_f\|x - \hat{x}\| \quad \forall x, \hat{x} \in \mathbb{R}^{12}
\tag{14}
$$

where L_f is a positive constant.

The following augmented system state space is obtained by considering actuator and sensor faults as auxiliary states.

$$\begin{aligned} \dot{\bar{x}} &= \bar{A}\bar{x} + \bar{\Phi}(A_0\bar{x}, t) + \bar{B}u + \bar{D}\bar{d} \\ y &= \bar{C}\bar{x} \end{aligned} \tag{15}$$

where

$$\bar{x} = \begin{bmatrix} x \\ f_a \\ f_s \end{bmatrix}, \quad \bar{A} = \begin{bmatrix} A & F_a & 0 \\ 0 & 0 & 0 \\ 0 & 0 & 0 \end{bmatrix}, \quad \bar{B} = \begin{bmatrix} B \\ 0 \\ 0 \end{bmatrix}, \quad \bar{D} = \begin{bmatrix} D & 0 & 0 \\ 0 & I_4 & 0 \\ 0 & 0 & I_6 \end{bmatrix}$$

$$\bar{C} = \begin{bmatrix} C & 0 & F_s \end{bmatrix}, \quad \bar{\Phi}(A_0\bar{x}, t) = \begin{bmatrix} \Phi(x,t) \\ 0 \end{bmatrix}, \quad \bar{d} = \begin{bmatrix} d \\ \dot{f}_a \\ \dot{f}_s \end{bmatrix}, \quad A_0 = \begin{bmatrix} I_{12} & 0 & 0 \end{bmatrix}$$

A NUIO estimates the augmented state $\bar{x}$ as follows:

$$\begin{aligned} \dot{z} &= Mz + Gu + N\bar{\Phi}(A_0\hat{\bar{x}}, t) + Ly \\ \hat{\bar{x}} &= z + Hy \end{aligned} \tag{16}$$

where $z \in \mathbb{R}^{22}$ is the observer system state and $\hat{\bar{x}} \in \mathbb{R}^{22}$ is the estimate of $\bar{x}$. The matrices $M \in \mathbb{R}^{22\times 22}$, $G \in \mathbb{R}^{22\times 4}$, $N \in \mathbb{R}^{22\times 22}$, $L \in \mathbb{R}^{22\times 12}$, and $H \in \mathbb{R}^{22\times 12}$ are to be designed.

The estimation error is stated as $e = \bar{x} - \hat{\bar{x}}$, it's time derivetive is given by:

$$\begin{aligned} \dot{e} &= (T\bar{A} - L_1\bar{C})e + (T\bar{A} - L_1\bar{C} - M)z + (T\bar{B} - G)u \\ &\quad + \left[(T\bar{A} - L_1\bar{C})H - L_2\right] y + T\bar{\Phi}(\bar{A}_0 x, t) - N\bar{\Phi}(\bar{A}_0\hat{x}, t) + T\bar{D}\bar{d} \end{aligned} \tag{17}$$

where $T = I_{22} - H\bar{C}$ and $L = L_1 + L_2$. The observer matrices M, G, N, and L_2 are given by:

$$M = T\bar{A} - L_1\bar{C}, \quad N = T, \quad G = T\bar{B}, \quad L_2 = (T\bar{A} - L_1\bar{C})H \tag{18}$$

Substituting (18) into (17), and assuming the effect of system nonlinearity on the FE observer is negligible, since this simplification allows for a more tractable analysis without significant loss of accuracy, the error dynamics become:

$$\dot{e} = (T\bar{A} - L_1\bar{C})e + T\bar{D}\bar{d} \tag{19}$$

In contrast to Studies [12]-[16], this work addresses the attenuation of disturbance using resilient design, rather than complete decoupling.

A sufficient requirement for the existence of a NUIO (16), is given by Theorem 1 below:

Theorem 1. *Given a positive scalar γ, the system error (19) is asymptotically stable with H_∞ performance $\|G_{z\bar{d}}\|_\infty < \gamma$, if there exists a symmetric positive definite matrix $P \in \mathbb{R}^{22\times 22}$, and matrices $M_1 \in \mathbb{R}^{22\times 12}$ and $M_2 \in \mathbb{R}^{22\times 12}$ such that*

$$\begin{bmatrix} \Omega_1 & \Omega_2 \\ \Omega_2^T & -\gamma^2 I_{16} \end{bmatrix} < 0 \tag{20}$$

where $\Omega_1 = He[P\bar{A} - M_1\bar{C}\bar{A} - M_2\bar{C}] + C_e^T C_e$ and $\Omega_2 = (P - M_1\bar{C})\bar{D}$. And $z = C_e e$ where $C_e \in \mathbb{R}^{22\times 22}$. And $He(V) = V + V^\top$ for a given matrix V.

Proof. Let's consider the following Lyapunov function

$$V_e = e^T P e \tag{21}$$

where e is by (19) and P is a symmetric positive definite matrix, then

$$\begin{aligned} \dot{V}_e &= \dot{e}^T P e + e^T P \dot{e} \\ &= e^T He[P(T\bar{A} - L_1\bar{C})]e + He[e^T P T\bar{D}\bar{d}] \end{aligned} \tag{22}$$

The H_∞ performance $\|G_{z\bar{d}}\|_\infty < \gamma$ is given by

$$J = \int_0^\infty \left(z^T z - \gamma^2 \bar{d}^T \bar{d}\right) dt < 0 \tag{23}$$

Under zero initial conditions, (23) becomes

$$\begin{aligned} J &= \int_0^\infty \left(z^T z - \gamma^2 \bar{d}^T \bar{d} + \dot{V}_e\right) dt - \int_0^\infty \dot{V}_e \, dt \\ &= \int_0^\infty \left(z^T z - \gamma^2 \bar{d}^T \bar{d} + \dot{V}_e\right) dt - (V_e(\infty) + V_e(0)) \\ &\leq \int_0^\infty \left(z^T z - \gamma^2 \bar{d}^T \bar{d} + \dot{V}_e\right) dt \end{aligned} \tag{24}$$

To satisfy (24), the following sufficient conditions are required:

$$J_1 = z^T z - \gamma^2 \bar{d}^T \bar{d} + \dot{V}_e < 0 \tag{25}$$

Substituting (22) into (26) yields

$$J_1 = z^T z - \gamma^2 \bar{d}^T \bar{d} + e^T \mathrm{He}[P(T\bar{A} - L_1\bar{C})]e + \mathrm{He}[e^T PT\bar{D}\bar{d}] \tag{26}$$

By defining $M_1 = PH$ and $M_2 = PL_1$, the condition (26) is satisfied if

$$\begin{bmatrix} \Omega_1 & \Omega_2 \\ \Omega_2^T & -\gamma^2 I_{16} \end{bmatrix} < 0 \tag{27}$$

where $\Omega_1 = \mathrm{He}[P\bar{A} - M_1\bar{C}\bar{A} - M_2\bar{C}] + C_e^T C_e$ and $\Omega_2 = (P - M_1\bar{C})\bar{D}$. □

Matrices P, M_1, and M_2 can be found by solving the LMI given by (27), then $H = P^{-1}M_1$ and $L_1 = P^{-1}M_2$. Matrices H and L_1 will be used to find matrices T, M, N, G, and L through the equations given by (18).

The linear matrix inequalities (LMIs) were solved using CVX, a MATLAB-based modeling system for convex optimization.

4 Backstepping Sliding Mode Fault-Tolerant Controller Design

The proposed control approach is based on two loops, the internal loop has four control laws (U_1, U_2, U_3, and U_4), and the external loop has two virtual control laws (U_x and U_y). The synoptic scheme (Figure 2) below illustrates this control strategy.

The synthesized stabilizing control laws are as described in the following:

$$U_2 = \frac{1}{b_1}\left[\ddot{\phi}_d - a_1x_4x_6 - a_2x_2^2 - a_3\bar{\Omega}x_4 - k_1\dot{e}_1 - A_1\dot{s}_1 - s_1 - A_2s_2 - \hat{f}_{a1} - \dot{\hat{f}}_{s1} - \hat{\Gamma}_1\mathrm{sign}(s_2)\right] \tag{28a}$$

$$U_3 = \frac{1}{b_2}\left[\ddot{\theta}_d - a_4x_7x_9 - a_5x_8^2 - a_6\bar{\Omega}x_7 - k_3\dot{e}_3 - A_3\dot{s}_3 - s_3 - A_4s_4 - \hat{f}_{a2} - \dot{\hat{f}}_{s2} - \hat{\Gamma}_2\mathrm{sign}(s_4)\right] \tag{28b}$$

$$U_4 = \frac{1}{b_3}\left[\ddot{\psi}_d - a_7x_7x_8 - a_8x_9^2 - k_5\dot{e}_5 - A_5\dot{s}_5 - s_5 - A_6s_6 - \hat{f}_{a3} - \dot{\hat{f}}_{s3} - \hat{\Gamma}_3\mathrm{sign}(s_6)\right] \tag{28c}$$

$$U_x = \frac{m}{U_1}\left[\ddot{x}_d - a_9x_{10} - k_7\dot{e}_7 - A_7\dot{s}_7 - s_7 - A_8s_8 - \dot{\hat{f}}_{s4} - \hat{\Gamma}_4\mathrm{sign}(s_8)\right] \tag{28d}$$

$$U_y = \frac{m}{U_1}\left[\ddot{y}_d - a_{10}x_{11} - k_9\dot{e}_9 - A_9\dot{s}_9 - s_9 - A_{10}s_{10} - \dot{\hat{f}}_{s5} - \hat{\Gamma}_5\mathrm{sign}(s_{10})\right] \tag{28e}$$

$$U_1 = \frac{m}{cx_1cx_2}\left[\ddot{z}_d - a_{11}x_{12} + g - k_{11}\dot{e}_{11} - A_{11}\dot{s}_{11} - s_{11} - A_{12}s_{12} + \hat{f}_{a4} - \dot{\hat{f}}_{s6} - \hat{\Gamma}_6\mathrm{sign}(s_{12})\right] \tag{28f}$$

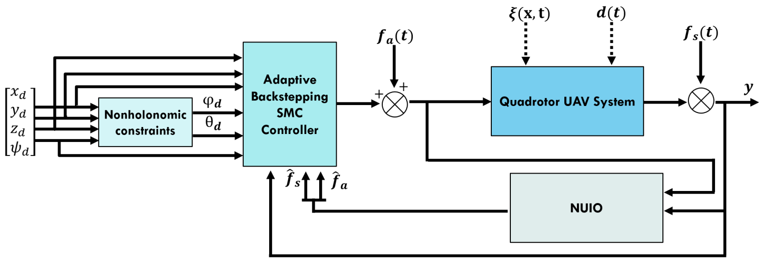

Figure 2: Synoptic scheme illustrating the control strategy.

Proof. Let's demonstrate the expression of U_2, considering the following roll subsystem:

$$\begin{cases} \dot{x}_1 = x_2 \\ \dot{x}_2 = \Phi_1 + b_1 U_2 + f_{a1} + d_\phi + \xi_\phi \end{cases} \tag{29}$$

where $\Phi_1 = a_1 x_4 x_6 + a_2 x_2^2 + a_3 \bar{\Omega} x_4$.

The output subsystem vector is given by $[y_1 \quad y_2 - f_{s1}] = [x_1 \quad x_2 - f_{s1}]$, where f_{s1} is a sensor fault.

Step 1: Define the control error as $e_1 = y_1 - y_{1d} = x_1 - x_{1d}$. The sliding surface equation is:

$$s_1 = e_1 + k_1 \int e_1 \, dt \qquad\qquad k_1 > 0 \tag{30}$$

The Lyapunov function chosen is:

$$V_1 = \frac{1}{2} s_1^2 \tag{31}$$

The time derivative of V_1 is:

$$\begin{aligned} \dot{V}_1 &= s_1 \dot{s}_1 = s_1(\dot{e}_1 + k_1 e_1) \\ &= s_1(y_2 + f_{s1} - \dot{x}_{1d} + k_1 e_1) \end{aligned} \tag{32}$$

The virtual control input is chosen as $(y_2)_d = \alpha_1 = \dot{x}_{1d} - k_1 e_1 - A_1 s_1 - \hat{f}_{s1} - \alpha_{s1}$. Where α_{s1} is a nonlinear damping remains to be determined.

Substituting the virtual control value of $(y_2)_d$, $\dot{V}_1$ becomes:

$$\dot{V}_1 = -A_1 s_1^2 - s_1(\alpha_{s1} - \tilde{f}_{s1}) \tag{33}$$

where $\tilde{f}_{s1} = f_{s1} - \hat{f}_{s1}$. Choosing $\alpha_{s1} = k_{s1}\, \mathrm{sign}(s_1)$, where $\mathrm{sign}(\cdot)$ denotes the sign function and $k_{s1} > 0$.

Equation (33) becomes:

$$\begin{aligned} \dot{V}_1 &= -A_1 s_1^2 - s_1 \left(k_{s1}\, \mathrm{sign}(s_1) - \tilde{f}_{s1}\right) \\ &\leq -A_1 s_1^2 - |s_1| \left(k_{s1} - |\tilde{f}_{s1}|\right) \end{aligned} \tag{34}$$

Suppose there exists a positive constant k_{s1}, such that $|\tilde{f}_{s1}| \leq k_{s1}$.

Finally, the equation (34) becomes

$$\dot{V}_1 \leq -A_1 s_1^2 \leq 0 \tag{35}$$

Step 2: The second sliding surface is:

$$s_2 = y_2 - \alpha_1 = y_2 - \dot{x}_{1d} + k_1 e_1 + A_1 s_1 + \hat{f}_{s1} + \alpha_{s1} \tag{36}$$

The derivative of s_2 over time is:

$$\dot{s}_2 = \Phi_1 + b_1 U_2 + f_{a1} + d_\phi + \xi_\phi - \dot{f}_{s1} - \ddot{x}_{1d} + k_1 \dot{e}_1 + A_1 \dot{s}_1 + \dot{\hat{f}}_{s1} + \dot{\alpha}_{s1} \tag{37}$$

Based on the principle of certain equivalence, f_{a1} and d_ϕ are replaced by their estimates. Using the sliding surface in equation (38), the input control U_2 is given by:

$$U_2 = \frac{1}{b_1} \left[\ddot{\phi}_d - \Phi_1 - k_1 \dot{e}_1 - A_1 \dot{s}_1 - s_1 - A_2 s_2 - \hat{f}_{a1} - \dot{\hat{f}}_{s1} - \hat{\Gamma}_1 \mathrm{sign}(s_2) \right] \tag{38}$$

where $\dot{\hat{\Gamma}}_1 = \beta_1|s_2|$, and β_1 is a positive constant. Replacing U_2 in equation (37), $\dot{s}_2$ becomes

$$\dot{s}_2 = \tilde{f}_{a1} + d_\phi + \xi_\phi - \dot{f}_{s1} - \dot{\alpha}_{s1} - s_1 - \hat{\Gamma}_1 \text{sign}(s_2) - A_2 s_2 \tag{39}$$

The presence of the terms $\tilde{f}_{a1}$, d_ϕ, ξ_ϕ, $\dot{f}_{s1}$, and $\dot{\alpha}_{s1}$ in the expression of $\dot{s}_2$ does not assert the system stability. To overcome this obstacle, we increase the function of Lyapunov by adding a square term involving $\tilde{\Gamma}_1$.

$$V_2 = \frac{1}{2}(s_1^2 + s_2^2) + \frac{1}{2\beta_2}\Gamma_2^2 \tag{40}$$

where $\tilde{\Gamma}_1 = \Gamma_1 - \hat{\Gamma}_1$, and $\hat{\Gamma}_1$ is the estimate of Γ_1 (assuming $\dot{\Gamma}_1 \approx 0$). Its derivative is

$$\begin{aligned}
\dot{V}_2 &= s_1\dot{s}_1 + s_2\dot{s}_2 + \frac{1}{\beta_1}\tilde{\Gamma}_1\dot{\hat{\Gamma}}_1 \\
&= s_1(s_2 - A_1 s_1) + s_2\dot{s}_2 - (\Gamma_1 - \hat{\Gamma}_1)|s_2| \\
&\leq -A_1 s_1^2 - A_2 s_2^2 + \hat{\Gamma}_1(|s_2| - s_2 \text{sign}(s_2)) + |s_2|(\tilde{f}_{a1} + d_1 + \xi_1 - \dot{f}_{s1} - \dot{\alpha}_{s1} - \Gamma_1) \\
&\leq -A_1 s_1^2 - A_2 s_2^2 + |s_2|(|\tilde{f}_{a1} + d_\phi + \xi_\phi - \dot{f}_{s1} - \dot{\alpha}_{s1}| - \Gamma_1)
\end{aligned} \tag{41}$$

Assumption 5: There exists an unknown parameter $\Gamma_1 > 0$, such that:

$$|\tilde{f}_{a1} + d_\phi + \xi_\phi + \dot{f}_{s1} - \dot{\alpha}_{s1}| \leq \Gamma_1 \tag{42}$$

Thus, $\dot{V}_2 \leq 0$ if $|\tilde{f}_{a1} + d_\phi + \xi_\phi + \dot{f}_{s1} - \dot{\alpha}_{s1}| \leq \Gamma_1$.

To avoid non-differentiability and chattering phenomena, the sign function will be replaced by a smooth function.

$$\text{sign}(s, \delta) = \frac{s}{\|s\| + \delta} \tag{43}$$

where δ is a small positive constant. □

5 Simulation Results and Analysis

To evaluate the performance of the proposed FTC, we executed simulations in the MATLAB-SIMULINK® environment across three scenarios. Scenario 1 involved trajectory tracking with only wind disturbances and uncertainties. Scenario 2 introduced actuator faults, wind disturbances, and uncertainties, while Scenario 3 included both actuator, sensor faults, wind disturbances, and uncertainties. The integration time step is chosen as 0.001s. The quadrotor subject of our study is the Draganfly IV manufactured by "Draganfly Innovations". Parameter identification is studied in [25].

For the Observer design purpose, choosing $Y_1 = 0.3 \cdot \mathbf{1}_{4\times12}$, $C_1 = I_{22}$, $\gamma = 0.5$, and $L_f = 35$.

In Simulink, the "Von Karman Wind Turbulence Model" block was used to produce time-varying wind gusts as output. In our models, the mean wind speeds are of 5 m/s for attitude and 8 m/s for position. The figure 3 illustrates the varying velocity of wind disturbances over time.

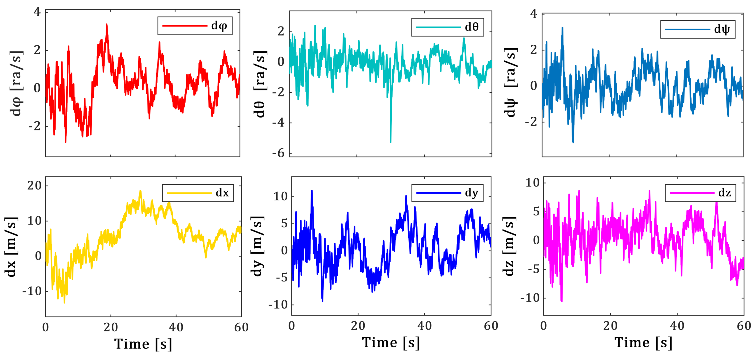

Figure 3: Wind disturbances velocity profile using Von Kármán model.

Table 1: Actuator faults f_{a1} and f_{a4} profile

$f_{a1}(\phi)$	$f_{a4}(z)$	Occurrence time	Fault type
0	0	$0 \leq t < 10$ s	Fault free
5	5	$10 \leq t < 20$ s	Bias fault
$-0.4U_2(t)$	$-0.3U_1(t)$	$20 \leq t < 30$ s	LOE
$-U_2(t)+5$	$-U_1(t)+5$	$30 \leq t < 40$ s	Actuator Stuck
$-U_2(t)-5$	$-U_1(t)-5$	$40 \leq t < 50$ s	Actuator Stuck
$2W(t)$	$1W(t)$	$50 \leq t < 60$ s	Weierstrass function

Assuming that K_{ftx}, K_{fty}, and K_{ftz}, as well as K_{fax}, K_{fay}, and K_{faz} are subject to a parametric uncertainty of 15% (for example, $\Delta K_{ftx} = 0.15K_{ftx}$).

The actuator fault profile is resumed in table 1. Where $W(t) = \sum_{k=0}^{5} 0.4^k \cos(3^k \pi t)$ is the Weierstrass function-type fault that is smooth but non-differentiable.

Additive Gaussian noise is added to the actuator faults. $\mathcal{N}_{a1}(0.05, 0.05^2)$ is added to f_{a1}, and $\mathcal{N}_{a4}(0.005, 0.005^2)$ is added to f_{a4}, with a sampling period of 0.05s for both.

The corresponding FE of f_{a1} and f_{a4} in each actuator is shown in Figure 4. It demonstrates good FE accuracy with RMSE (Root Mean Square Error) for f_{a1} (ϕ) and f_{a4} (z) hovering around 10^{-14}.

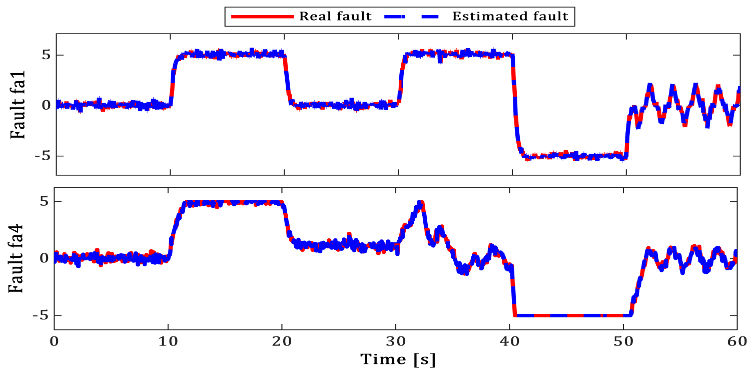

Figure 4: Actuator fault estimation.

The sensor fault profile with different sensor fault types occurring sequentially is described in table 2. Noise $\mathcal{N}_{s4}$=$\mathcal{N}_{s5}$=$(0.01, 0.01^2)$ is added to f_{s4} and f_{s5}, with a sampling period of 0.02s.

Table 2: Sensor faults f_{s1} (ϕ), f_{s4} (x), f_{s5} (y) profile

$f_{s1}(\phi)$	$f_{s4}(x)$	$f_{s5}(y)$	Occurrence time	Fault type
0	0	0	$0 \leq t < 10\,$s	Fault free
1	5	5	$10 \leq t < 20\,$s	Bias fault
$0.1t$	$0.6t$	$0.6t$	$20 \leq t < 30\,$s	Drift fault
$-0.6\dot{\phi}(t)$	$-0.25\dot{x}(t)$	$-0.25\dot{y}(t)$	$30 \leq t < 40\,$s	LOE fault
$-\dot{\phi}(t)+1$	$-\dot{x}(t)+5$	$-\dot{y}(t)+5$	$40 \leq t < 50\,$s	Stuck Sensor fault
$0.4W(t)$	$4W(t)$	$4W(t)$	$50 \leq t < 60\,$s	Weierstrass function fault

To test the robustness of the proposed technique, we examined the impact of a simultaneous actuator and sensor fault on the roll.

Sensor fault estimation of f_{s1}, f_{s4}, and f_{s5} is with RMSE performances remaining close to zero.

Figure 6 illustrates the system's tracking performance. Despite the presence of some fluctuations in the states, particularly in ϕ, x, and y, the tracking remains robust, showcasing the effectiveness of the proposed FTC strategy.

The figure 7 illustrates the global trajectory of the quadrotor in 3D along the (X, Y, Z) axis in the presence of actuator and sensor faults. Despite some fluctuations, it reveals a stable and accurate flight path, even with the challenges posed by faults.

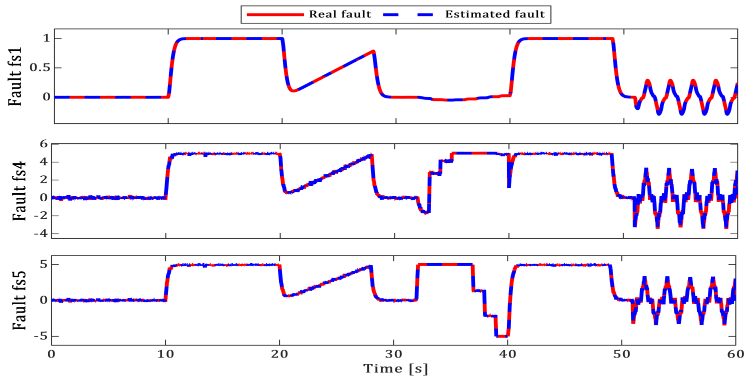

Figure 5: Sensor FE of f_{s1}, f_{s4}, and f_{s5}

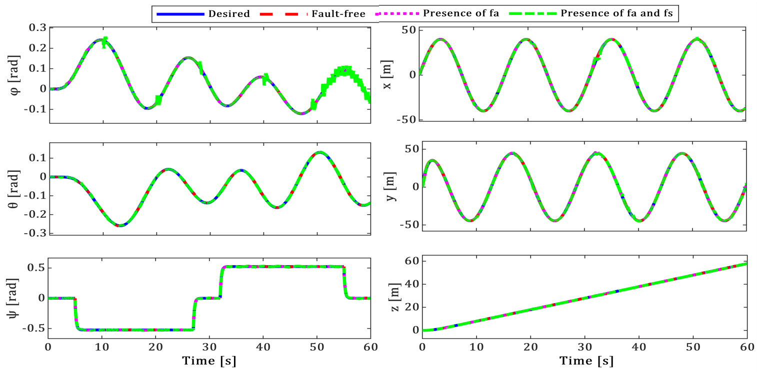

Figure 6: Trajectories along attitude and position in the presence of actuator and sensor faults

In Figure 8, the plots reveal that the tracking errors for θ, ψ, and z are small across all scenarios, while errors for ϕ, x, and y increase significantly in the presence of both actuator and sensor faults. Despite that, the attitude mean error remains below 10^{-5} rad and the position mean error stays under 10^{-3} m.

Figure 9 illustrates the control inputs U_1, U_2, U_3, and U_4 of our system in the presence of actuator and sensor faults. The control signals generated by this strategy are both physically realizable and robust, reflecting the practicality of the proposed FTC approach. Additionally, the low energy consumption is maintained through small control inputs.

The Table 3 comparing the RMSE for the three different scenarios provides valuable insights into the quadrotor's performance.

In Scenario 1, where only external disturbances and uncertainties are present, the system shows minimal deviation in both attitude and position of the RMSE. In Scenario 2, where actuator faults are introduced, the RMSE values remain nearly identical to those in Scenario 1, showing that the control

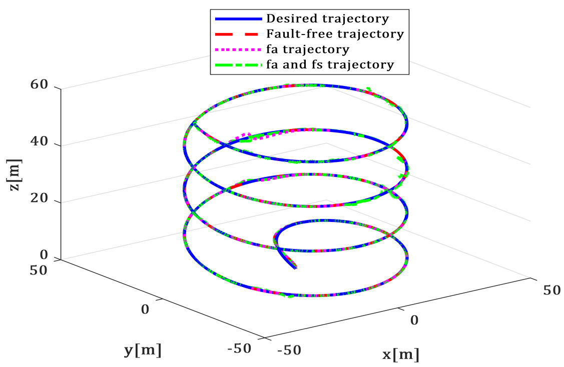

Figure 7: Global trajectory of the quadrotor in 3D in presence of actuators and sensor faults.

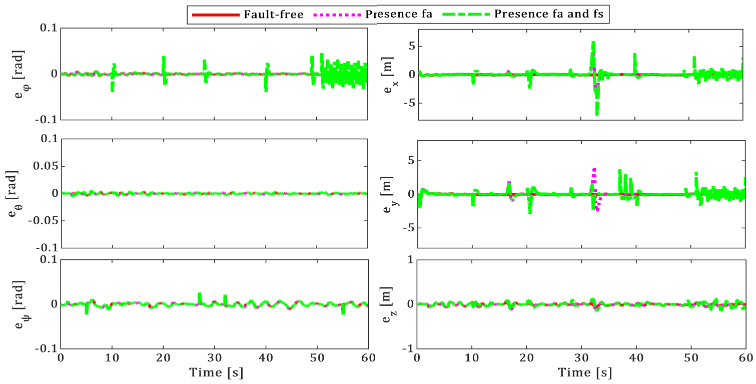

Figure 8: Tracking errors in the presence of actuator and sensor faults.

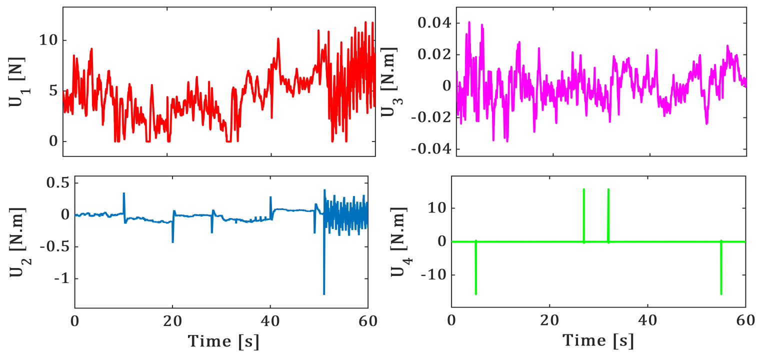

Figure 9: Control inputs of actuators in presence of actuator and sensor faults

Table 3: RMSE values for attitude (on rad) and position (on m) in different scenarios.

Scenario	**RMSE** (ϕ)	**RMSE** (θ)	**RMSE** (ψ)	**RMSE** (x)	**RMSE** (y)	**RMSE** (z)
Scenario 1	1.38×10^{-3}	1.45×10^{-3}	4.66×10^{-3}	1.22×10^{-3}	1.24×10^{-3}	2.44×10^{-2}
Scenario 2	1.38×10^{-3}	1.45×10^{-3}	4.66×10^{-3}	2.80×10^{-2}	2.75×10^{-2}	2.66×10^{-2}
Scenario 3	3.38×10^{-3}	1.45×10^{-3}	4.66×10^{-3}	0.15	0.16	2.80×10^{-2}

strategy is robust against actuator faults. In Scenario 3, both actuator and sensor faults are present. The attitude RMSE values remain nearly identical to those in Scenario 2. The x and y coordinates RMSE values increase, while the z coordinate RMSE remain nearly identical to those in Scenario 2.

6 Conclusion

This study begins with a short description of the quadrotor's nonlinear dynamic model, which takes into consideration the nonlinearities and high-order nonholonomic constraints of the system. In the presence of uncertainties and external disturbances, a novel NUIO is proposed to estimate actuator and sensor faults simultaneously, without requiring certain system matrices to have a specific rank to ensure that faults or disturbances can be isolated without ambiguity; the FE unit design problem is formulated as an observer-based robust control problem, and it is solved using H_∞ optimization in an LMI formulation. An adaptive backstepping sliding mode FTC controller using the NUIO-based FE is constructed. To evaluate the performance of the proposed controller, we executed simulations in MATLAB across three scenarios. Based on the analysis of three scenarios with different faults and disturbances, the proposed FTC system shows varying performance.

The results of the simulation clearly illustrate the good performance of the adopted strategy, as it made it possible to precisely estimate the faults and to ensure stability and trajectory tracking.

The proposed FTC techniques demonstrate robust performance in mitigating the effects of wind disturbances and uncertainties, maintaining acceptable tracking accuracy in various scenarios, and addressing different environmental challenges effectively.

References

[1] Baldini, A., Felicetti, R., Freddi, A., Monteriù, A., "Fault-Tolerant Control of a Variable-Pitch Quadrotor under Actuator Loss of Effectiveness and Wind Perturbations," *Sensors and Transducers*, vol. 23, no. 10, p. 4907, May 2013.

[2] Nguyen, N., Hong, S., "Fault-Tolerant Control of Quadcopter UAVs Using Robust Adaptive Sliding Mode Approach," *Energies*, vol. 12, p. 95, December 2018.

[3] Nguyen, N., Hong, S., "Active Fault-Tolerant Control of a Quadcopter against Time-Varying Actuator Faults and Saturations Using Sliding Mode Backstepping Approach," *Applied Sciences*, vol. 9, p. 4010, September 2019.

[4] Wang, B., Yu, X., Mu, L., Zhang, Y., "Disturbance observer-based adaptive fault-tolerant control for a quadrotor helicopter subject to parametric uncertainties and external disturbances," *Mechanical Systems and Signal Processing*, vol. 120, pp. 727-743, April 2019.

[5] Ma, H., Liu, Y., Li, T., Yang, G.-H., "Nonlinear High-Gain Observer-Based Diagnosis and Compensation for Actuator and Sensor Faults in a Quadrotor Unmanned Aerial Vehicle," *IEEE Transactions on Industrial Informatics*, vol. 15, no. 1, pp. 550-562, August 2019.

[6] Nguyen, N.-P., Pitakwatchara, P., "Attitude Fault-Tolerant Control of Aerial Robots with Sensor Faults and Disturbances," *Drones*, vol. 7, p. 156, February 2023.

[7] Ezzara, A., Ouadine, A. Y., Ayad, H., "Adaptive Observer-based Fault-Tolerant Control for Actuator Faults in Quadrotor UAV," in *2024 International Conference on Global Aeronautical Engineering and Satellite Technology (GAST)*, pp. 1-5, 2024.

[8] Ouadine, A. Y., Mjahed, M., Ayad, H., El Kari, A., "UAV Quadrotor Fault Detection and Isolation Using Artificial Neural Network and Hammerstein-Wiener Model," *Studies in Informatics and Control*, vol. 29, no. 3, pp. 317-328, 2020.

[9] Zou, P., Hou, B., Jiang, L., Zhang, Z.,"Bearing Fault Diagnosis Method Based on EEMD and LSTM,"*International Journal of Computers Communications and Control*, vol. 15, no. 1, 2020.

[10] Moldovan, O., Ghincu, R., Moldovan, A., Noje, D., Tarca, R., "Fault Detection in Three-phase Induction Motor based on Data Acquisition and ANN based Data Processing,"*International Journal of Computers Communications and Control*, vol. 17, no. 3, 2022.

[11] Lan, J., Patton, R. J., "Integrated fault estimation and fault-tolerant control for uncertain Lipschitz non-linear systems," *International Journal of Robust and Nonlinear Control*, vol. 27, no. 5, pp. 761-780, 2016.

[12] Gao, Z., Liu, X., Chen, M., "Unknown Input Observer Based Robust Fault Estimation for Systems Corrupted by Partially-Decoupled Disturbances," *IEEE Transactions on Industrial Electronics*, vol. 63, pp. 1-1, January 2015.

[13] Chen, J., Patton, R., Zhang, H.-Y., "Design of unknown input observers and robust fault detection filters," *International Journal of Control*, vol. 63, pp. 85-105, February 2007.

[14] Chen, W., Saif, M., "Unknown input observer design for a class of nonlinear systems: An LMI approach," in *Proceedings of the American Control Conference*, vol. 2006, pp. 5 pp.-, July 2006.

[15] Xia, J., Jiang, B., Zhang, K., "UIO-Based Practical Fixed-Time Fault Estimation Observer Design of Nonlinear Systems," *Symmetry*, vol. 14, p. 1618, August 2022.

[16] Hashemi, M., Egoli, A., Naraghi, M., Tan, C., "Saturated Fault Tolerant Control Based on Partially Decoupled Unknown-Input Observer: A New Integrated Design Strategy," *IET Control Theory and Applications*, July 2019.

[17] Bouadi, H., Tadjine, M., Bouchoucha, M., "Modelling and stabilizing control laws design based on backstepping for an UAV type-quadrotor," *IFAC Proceedings Volumes*, vol. 40, no. 15, pp. 245-250, 2007.

[18] Li, F., Song, W.-P., Song, B., Jiao, J., "Dynamic Simulation and Conceptual Layout Study on a Quad-Plane in VTOL Mode in Wind Disturbance Environment," *International Journal of Aerospace Engineering*, vol. 2022, pp. 1-24, January 2022.

[19] Li, F., Song, W.-P., Song, B., Zhang, H., "Dynamic modeling, simulation, and parameter study of electric quadrotor system of Quad-Plane UAV in wind disturbance environment," *International Journal of Micro Air Vehicles*, vol. 13, January 2021.

[20] Cole, K., "Reactive trajectory generation and formation control for groups of UAVs in windy environments," Washington, 2018.

[21] Boskovic, J., Mehra, R., "Stable adaptive multiple model-based control design for accommodation of sensor failures," in *Proceedings of the American Control Conference*, vol. 3, pp. 2046 - 2051, February 2002.

[22] Jinghui, P., Lili, Q., Kaixiang, P., "Sensor and Actuator Fault Diagnosis for Robot Joint Based on Deep CNN," *Entropy*, vol. 23, p. 751, June 2021.

[23] Balaban, E., Saxena, A., Bansal, P., Goebel, K. F., Curran, S., "Modeling, Detection, and Disambiguation of Sensor Faults for Aerospace Applications," *IEEE Sensors Journal*, vol. 9, no. 12, pp. 1907-1917, 2009.

[24] Silva, J., Saxena, A., Balaban, E., Goebel, K., "A knowledge-based system approach for sensor fault modeling, detection and mitigation," *Expert Systems with Applications*, vol. 39, pp. 10977-10989, September 2012.

[25] Derafa, L., Madani, T., Benallegue, A., "Dynamic modelling and experimental identification of four rotor helicopter parameters," in *2006 IEEE International Conference on Industrial Technology*, pp. 1834-1839, 2006.

Cite this paper as:

Ezzara, A.; Ouadine, A.Y.;Ayad, H. (2024). Adaptive-Backstepping-Sliding-Mode Fault-Tolerant Control of Quadrotor UAV in presence of external disturbances, uncertainties, and Simultaneous Actuator and Sensor faults,*International Journal of Computers Communications* & *Control*, 19(1), 4xyz, 2024.
https://doi.org/10.15837/ijccc.2024.1.4xyz